Physics of Compaction of Fine Cohesive Particles

A. Castellanos, J. M. Valverde, and M. A. S. Quintanilla

Departamento de Electronica y Electromagnetismo, Universidad de Sevilla, Avenida Reina Mercedes s/n, 41012 Sevilla, Spain

(Received 9 November 2004; published 22 February 2005)

Fluidized fractal clusters of fine particles display critical-like dynamics at the jamming transition, characterized by a power law relating consolidation stress with volume fraction increment [$\hat{\sigma}_c \propto (\Delta\phi)^{\beta}$]. At a critical stress clusters are disrupted and there is a crossover to a logarithmic law ($\Delta\phi = \nu \log\hat{\sigma}_c$) resembling the phenomenology of soils. We measure $\lambda \equiv -\partial\Delta(1/\phi)/\partial\log\hat{\sigma}_c \propto \mathrm{Bo}_g^{0.2}$, where Bo_g is the ratio of interparticle attractive force (in the fluidlike regime) to particle weight. This law suggests that compaction is ruled by the internal packing structure of the jammed clusters at nearly zero consolidation.

DOI: 10.1103/PhysRevLett.94.075501 PACS numbers: 61.43.Gt, 45.70.Cc, 61.43.Hv, 81.20.Ev

Empirical studies on the compaction of soils date back to the beginning of the last century. Walker [1] fitted his data by the logarithmic law $\Delta(1/\phi) = -\lambda\log(\sigma_c/\sigma_{c0})$, where ϕ is the particle volume fraction, σ_c the applied consolidation stress, and λ (compression index) and σ_{c0} are empirical parameters. This equation applies well in loose samples, where compaction is driven by rearrangement of particles, and has been traditionally used in civil engineering [2,3]. An essential ingredient in most granular systems is cohesion. Tests on cohesive powders show that λ decreases with the particle volume fraction of the initial state [4,5], indicating that interparticle attractive forces, which favor the formation of porous structures, play a relevant role in the compaction process. Yet the initial state in typical engineering experiments involves consolidation stresses $\sigma_{c0} > \sim 10$ kPa [5]. Many industry applications demand research on smaller consolidations as these correspond to conditions of powder flow. For example, in the handling of xerographic toners, typical consolidations range from a few pascals to a few hundred pascals. Moreover, experiments at low consolidations have a fundamental interest in order to characterize the transition from the fluidlike to the solidlike state (jamming) [6] since the structural properties of the unconsolidated jammed state ($\sigma_c \simeq 0$), which is the truly initial state in any compaction process, are determinant on the rearrangement of the further loaded particles. We study the compaction of fine particles with controlled attractive force, initially fluidized and later subjected to loads from just a few pascals up to 10 kPa. Our novel experimental study is aimed to shed light on the role of the initial state, i.e., the unconsolidated jammed state, on compaction. The powders tested are xerographic toners based on polymer (particle density $\rho_p \simeq 1$ g/cm^3). They are produced by an attrition process, thus having an irregular shape, and size classified in a range of particle sizes (d_p) from 19.1 to 7 μm by aerodynamic classification, showing a narrow particle size distribution (see Fig. 1). Additionally, the powders are blended with fumed silica nanoparticles (either 8 or 40 nm nominal diameters) to coat uniformly the polymer particle surface in concentrations from 10% to 100% of surface area coverage (SAC).

In the fluidized regime there is an attractive force F_0 between the dry and uncharged particles mainly arising from the van der Waals interaction $F_0 = F_{\mathrm{vdW}} \simeq A d_a/(24 z_0^2)$, where $z_0 \simeq 4$ Å is the distance of closest approach between two molecules, A is the Hamaker constant, and d_a is the typical size of the surface asperities (typically $A \sim 10^{-19}$ J and $d_a \sim 0.2$ μm) [7]. An estimation of electrostatic forces from charge spectrograph measurements shows that they are much smaller than van der Waals forces as commonly accepted in the literature for electroneutral fine powders [7,8]. A dry nitrogen atmosphere minimizes also capillary forces. Because of the strong interparticle attractive force as compared to particle weight, toner particles are clustered in the fluidlike regime [9]. According to our previous experimental results the typical number of particles per cluster N and typical ratio of cluster size to particle size κ depend on the ratio of attractive force to particle weight $F_0/(m_p g) \equiv \mathrm{Bo}_g$ (granular Bond number). In particular we found $N \sim \mathrm{Bo}_g^{\alpha}$ ($\alpha \simeq 0.7$) and $D = \ln N/\ln\kappa \simeq 2.5$ for the fractal dimension, in agreement

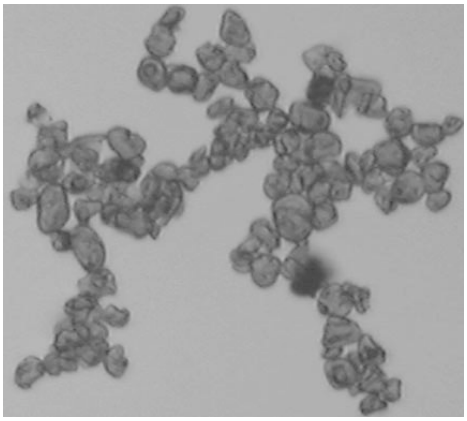

FIG. 1. Typical picture from the optical microscope of toner particles clustered in a nonaqueous liquid suspension that reminds one of a diffusion-limited aggregate. For this toner (12.7 μm particle size and 10% SAC) the fractal dimension obtained from settling experiments in gas fluidization [9] is $D \simeq 2.53$.

with the diffusion-limited-aggregation (DLA) model prediction. The typical size of surface asperities at contact can be decreased down to the size of silica agglomerates covering the particle surface for large enough SAC, thus reducing F_{vdW}. (From scanning electron miscrosopy micrographs we observe silica agglomerates of typical size $d_a \simeq 50$ nm for 8 nm silica nanoparticles and $d_a \simeq 200$ nm for 50 nm silica nanoparticles.) Since our fine particles are athermal, the limits to cluster growth in the initial fluidized state result from the interplay of gravitational and flow shear effects [10]. In order to estimate the limit size of our DLA clusters we will adopt a similar approach to that used in Ref. [11], where the limits to gelation in colloidal aggregation were studied. In the fluidized bed the weight of the cluster is balanced by the hydrodynamic drag from the surrounding gas. Fractal clusters screen external fields very effectively and the fluid flow inside the cluster is negligible compared to the flow outside, thus the drag acts mainly at the surface of the cluster whereas gravity is a body force acting uniformly through the cluster. This results in shear forces distributed across the cluster limiting its size. Using a simple spring model for the cluster, it has been shown [10,11] that the typical strain on the cluster is $\gamma \sim N m_p g/(K_c R_c)$, where K_c is the cluster spring constant and $R_c = \kappa d_p/2$ is the cluster radius. K_c is given by k_0/κ^β, where k_0 is the interparticle force constant, and the elasticity exponent is $\beta = 3$ in the 3D case [12]. Thus the local shear force inside the cluster is $F_s \sim k_0 \gamma d_p/2 \sim (m_p g)\kappa^{D+2}$. Manley *et al.* [11] use a critical value, measured independently, for the maximum strain sustainable to calculate the maximum size of their aggregates. More generally, we may estimate that the critical shear force must be of order of the interparticle attractive force $F_s^{\max} \sim F_0$, which leads to $\mathrm{Bo}_g \sim \kappa^{D+2}$, thus the maximum number of particles per cluster should be $N = \kappa^D \sim \mathrm{Bo}_g^{D/(D+2)}$. For DLA clusters ($D = 2.5$) we obtain $N \sim \mathrm{Bo}_g^{0.6}$, in close agreement with our previous experimental results [9]. Now we can explain why, for a constant F_0 (constant SAC), the size of our clusters measured in Ref. [9] was weakly dependent on particle size since the criterion predicts $k d_p \propto d_p^{0.3}$. Moreover, for our typical clusters ($\kappa < 10$) the intercluster Bond number is $\mathrm{Bo}_g^* = \mathrm{Bo}_g/N \sim \kappa^2 < 100$, i.e., intercluster cohesiveness is small.

In the experimental part of our work we use the fluidized bed tester to measure ϕ as a function of σ_c. A detailed report about the functioning of this apparatus can be found in Ref. [13]. A dry nitrogen serves to control σ_c, being pumped upward or downward through the powder bed while the gas pressure drop Δp across the bed is read from a differential pressure transducer. ϕ is derived from the height of the bed, which is measured by means of an ultrasonic sensor. In order to subject the powder to very low stresses, like in microgravity, the bed is allowed to settle under a small upwards directed gas flow. In this way σ_c is lowered down to $\sigma_c = W - \Delta p$, where W is the powder weight per unit area and Δp increases as the value of the decompressing gas flow used is larger. In Fig. 2 we have plotted ϕ near the jamming transition as a function of σ_c for toner Canon CLC700 (100% SAC, in this commercial toner the additive is TiO_2) and for an experimental toner with similar particle size (7.8 μm) but only 32% SAC. The jamming transition is discussed in detail in a previous work [14]. As seen in the data depicted in Fig. 2, it was generally observed that in a range of very small stresses the ϕ vs σ_c relationship follows a critical-like functional form $\sigma_c \propto (\phi - \phi_J)^\beta$, predicted by simulations [15] and reminiscent of an equilibrium critical phenomena.

In our new experimental study consolidation stresses larger than W are applied by a downwards directed gas flow. σ_c is thus increased up to $\sigma_c = W + \Delta p$. We see in Fig. 2 that the increment of ϕ as σ_c is increased deviates from the critical-like power law, and at a critical stress $\sigma_{c0} \sim 10$ Pa crosses over to a logarithmic law $\phi \simeq \phi_J + \nu \log \hat{\sigma}_c$ ($\hat{\sigma}_c \equiv \sigma_c/\sigma_{c0}$) remarkably similar to the empirical equation usually employed to describe the compaction of granular materials such as soils [2] in the rearrangement regime. Likely at $\hat{\sigma}_c \simeq 1$ clusters have reached their closest random packing (ϕ^*_{RCP}). The crossover to the logarithmic law occurs for volume fractions of clusters smaller than 0.64 (random close packing of noncohesive hard spheres) as it might be expected from the existence, although small, of intercluster cohesiveness. For example, $\phi^*_{\mathrm{RCP}} \simeq 0.53 \pm$

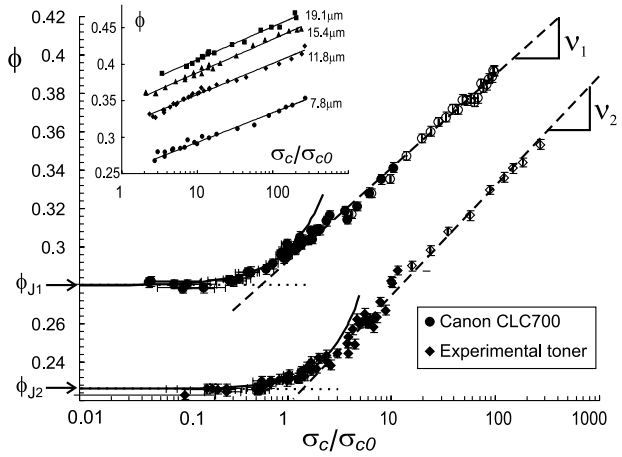

FIG. 2. Particle volume fraction as a function of the consolidation stress. Data obtained by consolidating the powder allowing it to settle under upward directed gas flows (solid symbols) are jointly plotted with data obtained by consolidating the powder by means of a downward directed gas flow (open symbols). Data correspond to commercial toner Canon CLC700 (100% SAC) and to an experimental toner with reduced surface additive coverage (32% SAC) and similar particle size. The lines correspond to the power law $\sigma_c \propto (\phi - \phi_J)^\beta$ that fits to the data in a range $\sigma_c \lesssim \sigma_{c0} = 10$ Pa and to a logarithmic fit $\phi - \phi_J \simeq \nu \log(\sigma_c/\sigma_{c0})$ that fits to the data in the range $\sigma_c \gtrsim \sigma_{c0}$. Inset: data in the logarithmic region for toners with the same SAC (32%) but different particle size (indicated).

0.02 for clusters of primary particle size from 7.8 to 19.1 μm and 32% SAC (see Fig. 4 in Ref. [14]), matching the reported value [16] for spheres of equivalent size to these clusters ($kd_p \simeq 50$ μm). The inset of Fig. 2 shows data for these toners with the same SAC (32%) but different particle size. It is observed that $\nu \simeq 0.04$ is almost independent of particle size, slightly decreasing when the SAC is increased (see main graph). Thus the correlation between ν and Bo_g seems to be at least a second order effect (note that a decrease of d_p from 19.1 to 7.8 μm covers a wide range of Bo_g). However, the data reported in the engineering literature reveal clear correlations between $\lambda = -\partial\Delta(1/\phi)/\partial\log\hat{\sigma}_c$ and the particle volume fraction of the lowest consolidation state. We plot in the inset of Fig. 3 the data for the same toners (32% SAC) of $1/\phi$ vs $\hat{\sigma}_c$, which are also well fitted to a logarithmic law $1/\phi \simeq 1/\phi_J - \lambda\log\hat{\sigma}_c$. The main graph shows λ as a function of Bo_g (calculated assuming $F_0 \sim F_{\mathrm{vdW}}$). A power law $\lambda \simeq 0.1\mathrm{Bo}_g^{0.21}$ is clearly seen. The extrapolated value for $\mathrm{Bo}_g = 1$ ($\lambda \simeq 0.1$) matches the typical value reported for noncohesive granular materials ($\mathrm{Bo}_g \lesssim 1$) such as sand [3]. What is the physical origin of this law? In a first order approach we may approximate $\Delta(1/\phi) \simeq [\partial(1/\phi)/\partial\log\hat{\sigma}_c]_J\log\hat{\sigma}_c \simeq -(1/\phi_J)^2\nu\log\hat{\sigma}_c$, where $\nu \simeq [\partial\phi/\partial\log\hat{\sigma}_c]_J$. Thus $\lambda \simeq (1/\phi_J)^2\nu$. Let us write $\phi_J \simeq \phi^*_{\mathrm{RCP}}\phi^c$, where $\phi^c = N/\kappa^3 = \kappa^{D-3}$ is the particle volume fraction within each cluster. Then $\lambda \simeq (1/\phi^*_{\mathrm{RCP}})^2\nu\mathrm{Bo}_g^{(6-2D)/(D+2)} = (1/\phi^*_{\mathrm{RCP}})^2\nu\mathrm{Bo}_g^{0.22}$, where we have used the cluster size limit criterion ($\mathrm{Bo}_g \sim \kappa^{D+2}$), and $D = 2.5$. Clusters behave as low cohesive effective spheres and thus ϕ^*_{RCP} will be almost independent on Bo_g. Using $\nu \simeq 0.04$ and $\phi^*_{\mathrm{RCP}} \simeq 0.53$ for the toners with 32% SAC, we would predict $\lambda \simeq 0.14\mathrm{Bo}_g^{0.22}$, in good agreement with the experimental result. We plot in Fig. 4 the data for λ vs Bo_g for other toners with SAC $> 30\%$ for which we admit $F_0 = F_{\mathrm{vdW}}$. The new data also scale with Bo_g in accordance with the predicted law. In summary, this law emphasizes the fundamental role of size and fractal structure of the jammed clusters on the distribution of voids to be filled in the compaction process. The case of highly cohesive powders (SAC $< 30\%$) needs, however, additional discussion. In the inset of Fig. 4 we include data for highly cohesive toners with only 20% SAC using $F_0 = F_{\mathrm{vdW}}$ to calculate Bo_g. The particle size for these toners is $\simeq 7$ μm and the base polymer is polyester treated with different amounts of a cross-linking agent (gel) that produces a slight increase of the polymer hardness (in any case small compared with the effect of silica). The data deviate clearly from the scaling law, showing unexpectedly large values of λ that must indicate the existence of large clusters. Moreover, in spite of the similar values of Bo_g (same particle weight and same van der Waals force: $A \simeq 10^{-19}$ J,

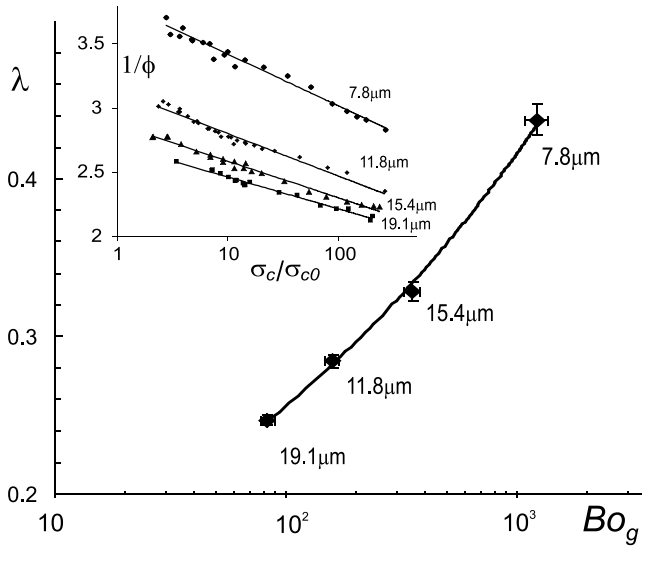

FIG. 3. Compression index versus the granular Bond number for toners with the same surface additive coverage (32% SAC) and varying particle size (indicated). The continuous line is a power law fit to the data ($\lambda \simeq 0.1\mathrm{Bo}_g^{0.21}$). Inset: inverse of particle volume fraction versus the consolidation stress, where lines are logarithmic fits to the data ($\sigma_{c0} = 10$ Pa).

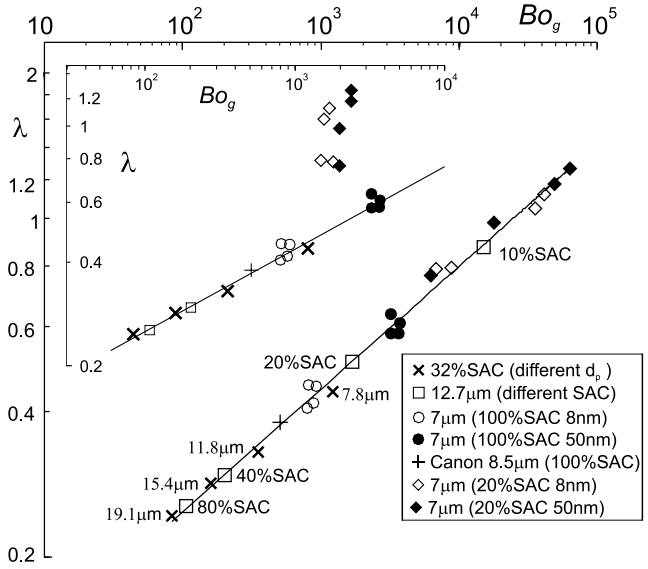

FIG. 4. Compression index versus granular Bond number for toners with different particle size and % SAC (indicated). In the main graph Bo_g is calculated assuming that the interparticle attractive force in fluidization is the van der Waals force for SAC $> 30\%$, while contact memory (see text) is considered for toners with SAC $< 30\%$. In the inset the van der Waals force is used for all the toners. For toners with 20% and 100% SAC, the effect of increasing the size of silica nanoparticle additives from 8 to 50 nm has been tested. Additionally, four different amounts of cross-linking agent in the parent polymer (from 0% to 45%) have been used in these toners. The continuous lines are power law fits to the data, only for toners with SAC $> 30\%$ in the inset ($\lambda \propto \mathrm{Bo}_g^{0.24}$) and for the whole set of toners in the main graph ($\lambda \propto \mathrm{Bo}_g^{0.25}$).

$d_a \simeq 0.2\ \mu$m), there is a clear difference between the compression indexes of toners with different gel content.

Silica additives improve powder flowability mainly by increasing the local hardness H on the contact as it is proven by the better flowability of toners blended with 200 nm silica agglomerates, of similar size to the typical polymer asperity size. The strong attractive forces between loaded fine particles cause plastic deformation of contacts, leading to a relevant increase of the adhesive force with the applied load [17]. Toners either without or with low percentage of the hard silica additive have a very poor flowability because it is difficult to break interparticle contacts between previously loaded particles, i.e., the interparticle contacts in highly cohesive powder will preserve the memory of the initial loaded state. It is likely that fragments that earlier existed as aggregates in the loaded powder persist in fluidization giving rise to large clusters of strongly adhered particles (a similar phenomenon has been recognized in fragmentation of colloidal suspensions of strongly cohesive particles [18]). Thus the attractive force between clustered particles in fluidization for these powders must be much larger than the van der Waals force. The increased contact hardness by silica additive reduces the rate of increase of the adhesive force with load [17], thus allowing for an easy breaking of interparticle contacts by an external energy source (such as gas fluidization), and therefore improving flowability. For these low cohesive toners the van der Waals force was indeed a good approximation to the interparticle attractive force in fluidization. For toners with only 20% SAC many contacts are between polymer surfaces. The rate of increase of the adhesive force with load increases as H is increased [17], which means that contacts with smaller hardness will give rise to larger clusters and thus to larger values of λ. (This explains the effect of gel seen on λ.) The problem is, How can we estimate Bo_g for these highly cohesive toners with hardness dependent memories? One possibility is to use the criterion for cluster limit size in fluidization, $\mathrm{Bo}_g \sim \kappa^{D+2}$, where $D \simeq 2.5$ according to sedimentation tests [9], and κ may be obtained from the information on the initial jammed state: $\kappa^D/\kappa^3 = \phi_J/\phi_J^*$. In this equation the most important and variable parameter is ϕ_J, which is accurately obtained from the logarithmic fit equation $\phi_J \approx \phi - \nu \log\hat{\sigma}_c$, while ϕ_J^* can be expected to show a small variation between $\sim$0.5 (10% SAC) and $\sim$0.55 (above 60% SAC). For low cohesive toners (SAC $\gtrsim$ 30%), the estimated Bo_g in this way is similar to the previously calculated one assuming $F_0 = F_{\mathrm{vdW}}$, but, for the highly cohesive ones, Bo_g is significantly larger as we anticipated. The main graph of Fig. 4 includes the data for 20% and 10% SAC toners with the new estimation of Bo_g, showing a good fit to the predicted power law. We can also discriminate now between the compression indices for 20% SAC toners in the base of the memory erasing effect of the cross-linking agent added to the parent polymer.

To conclude, we have investigated the compaction behavior of cohesive particles which are clustered in the fluidlike regime. The number of particles in our DLA clusters, and thus the cluster packing fraction (ϕ^c), is controlled by the ratio of the interparticle attractive force to particle weight Bo_g ($\phi^c \simeq \mathrm{Bo}_g^{-0.1}$). In the close vicinity of jamming and above a critical stress $\sigma_{c0} \sim 10$ Pa, there is a crossover to the logarithmic law $1/\phi \simeq 1/\phi_J - \lambda \log(\sigma_c/\sigma_{c0})$. Experimental studies in the engineering literature have usually shown this behavior, and the compression index λ has been correlated to the minimum particle volume fraction (corresponding to the smaller stress applicable, typically 10 kPa); the larger it is, the larger the λ. Our fluidization technique allows for a study of compaction behavior from just a few pascals, thus we are able to relate λ to the truly initial state of rearrangement. The initial distribution of voids to be filled, which rules the compaction process, is mainly determined by the internal packing structure of clusters that are jammed at the initial unconsolidated state. In a first order analysis we estimate $\lambda \propto (1/\phi_J^c)^2 \simeq \mathrm{Bo}_g^{0.2}$, in agreement with our measurements. Our analysis implies also that, due to the high plasticity of interparticle contacts in highly cohesive powders, these powders must retain memory in fluidization of previous loaded states; when jammed, very large clusters produce very porous initial states and as a consequence large values of the compression index.

We acknowledge the Xerox Foundation and the Spanish Ministerio de Ciencia y Tecnologia (Contract No. BMF2003-01739).

[1] E. E. Walker, Trans. Faraday Soc. **19**, 73 (1923).
[2] J. Atkinson, *The Mechanics of Soils and Foundations* (McGraw-Hill, London, 1993).
[3] P. Evesque, Poudres and Grains **10**, 6 (1999).
[4] D. Poquillon *et al.*, Powder Technol. **126**, 65 (2002).
[5] J. H. Park and T. Koumoto, J. Geotech. Geoenviron. Eng. **130**, 223 (2004).
[6] J. M. Valverde *et al.*, Phys. Rev. Lett. **86**, 3020 (2001).
[7] K. Rietema, *The Dynamics of Fine Powders* (Elsevier, London, 1991).
[8] H. Krupp, Adv. Colloid Interface Sci. **1**, 111 (1967).
[9] A. Castellanos *et al.*, Phys. Rev. E **64**, 041304 (2001).
[10] Y. Kantor and T. A. Witten, J. Phys. Lett. **45**, L675 (1984).
[11] S. Manley *et al.*, Phys. Rev. Lett. **93**, 108302 (2004).
[12] Y. Kantor and I. Webman, Phys. Rev. Lett. **52**, 1891 (1984).
[13] J. M. Valverde *et al.*, Rev. Sci. Instrum. **71**, 2791 (2000).
[14] J. M. Valverde *et al.*, Phys. Rev. Lett. **92**, 258303 (2004).
[15] C. S. O'Hern *et al.*, Phys. Rev. E **68**, 011306 (2003).
[16] R. Y. Yang *et al.*, Phys. Rev. E **62**, 3900 (2000).
[17] M. A. S. Quintanilla *et al.*, Phys. Rev. E **64**, 031301 (2001).
[18] Y. Tatek *et al.*, Powder Technol. **143–144**, 117 (2004).